arXiv:cond-mat/9908017v2 [cond-mat.str-el] 20 Dec 1999

Magnetization Process in the One-Dimensional Doped Kondo Lattice Model

Shinji Watanabe*
Department of Physics, Tohoku University, Sendai 980-8587

(July 28, 1999)

The magnetization process in the one-dimensional Kondo lattice model for the doped ($n_c < 1$) case is studied by the density matrix renormalization group method. A rapid increase of the magnetization is caused by the collapse of the intersite incommensurate correlation of f spins. On the contrary, the intrasite f-c singlet correlation survives in the larger magnetic field. The crossover from large to small Fermi surfaces for majority and minority spins is observed, whereas the Fermi surfaces are always contributed by f spins. A magnetization plateau appears with the magnitude of $1 - n_c$. Both ends of the plateau are related to the coherence temperature and the Kondo temperature which are characteristic energies essential in heavy electron systems.

PACS numbers: 71.10.Fd, 75.30.Mb

In heavy electron systems, metamagnetism has been attracting great interest for a long time. A typical compound CeRu$_2$Si$_2$ shows metamagnetic behavior at the magnetic field $H_\mathrm{M} = 7.7$ T [1]. In a de Haas-van Alphen (dHvA) experiment, the size of the Fermi surface changes at H_M [2]. According to band structure calculations [3], the measured Fermi surface is consistent with the itinerant f-electron band with the large Fermi surface below H_M. On the contrary, above H_M the measured Fermi surface is small, which is explained by the band structure of LaRu$_2$Si$_2$; f electrons seem to be localized. In a neutron measurement, the incommensurate spin correlation disappears rapidly around H_M, but spin fluctuation on the single site survives above H_M [4].

In the course of understanding above physics, it is a necessary step to exhibit a fundamental mechanism of the magnetization process in the basic model describing heavy electron systems. So far, numerical calculations for small clusters with a magnetization have been done in the periodic Anderson model (PAM) and the Kondo lattice model (KLM) [5–9]. However, the unified picture of the magnetization process in the whole range of the magnetic field has not been established yet even in the basic models.

The purpose of this Letter is to clarify the fundamental mechanism of the magnetization process in the basic model on the basis of an accurate method: We calculate the magnetization, Fermi surfaces and correlation functions in the one-dimensional KLM with use of the density matrix renormalization group (DMRG) method [10]. We show that the magnetization plateau is related to two characteristic energies essential in heavy electron systems. We also present the real-space picture and the band picture with respect to the quasi particle by comparing the magnetization process of the KLM with that of the PAM.

The one-dimensional KLM in a magnetic field is

$$H = -t\sum_{i\sigma}(c_{i\sigma}^\dagger c_{i+1\sigma} + \mathrm{H.c.}) + J\sum_i \mathbf{S}_i^f \cdot \mathbf{S}_i^c - h\sum_i \left(S_i^{fz} + S_i^{cz}\right), \qquad (1)$$

where $c_{i\sigma}^\dagger(c_{i\sigma})$ is a creation (annihilation) operator of a conduction electron on the i-th site ($1 \le i \le L$) with spin σ. $\mathbf{S}_i^f$ and $\mathbf{S}_i^c$ are spin operators on the i-th site of the f spin and the conduction electron, respectively. The rescaled magnetic field denoted by h includes the g-factor and the Bohr magneton μ_B. The magnetization is defined by $m \equiv n_\uparrow^f - n_\downarrow^f + n_\uparrow^c - n_\downarrow^c$, where n_σ^f and n_σ^c are the densities of f spins and conduction electrons with spin σ, respectively. The magnetization is related to $S_\mathrm{tot}^z = \sum_i(S_i^{fz} + S_i^{cz})$ as $m = 2S_\mathrm{tot}^z/L$ and m takes the range of $0 \le m \le 1 + n_c$.

We study the magnetization process of eq. (1) away from half filling ($n_c = n_\uparrow^c + n_\downarrow^c < 1$). In the DMRG calculation, we typically set the system size $L = 40$ under the open boundary condition and the number of states kept is taken up to 300.

As for the doped case at $h = 0$, a ferromagnetic metallic phase is known to exist in the large-J/t regime [12]. In this Letter we restrict to the paramagnetic metallic ground state without h. Figure 1 shows the magnetization process for $t = 1$ and $J = 1$ at $n_c = 4/5$. A plateau appears with the magnitude of $m = 1/5$ as seen near the left end of Fig. 1(a) (the enlargement will be given in Fig. 3). The magnetic field of the left (right) end of the plateau is denoted by $h_0(h_1)$. As n_c approaches 1, h_1 increases and continuously connects to the spin gap Δ_s at half filling without h; Δ_s is associated with the characteristic energy scale called Kondo temperature T_K [11]. In order to illustrate the constituents of the magnetization, the average for the z-component of spin is shown in Fig. 1(b). It turns out that the main component of the magnetization for $0 \le h \le h_0$ comes from f spins. The rapid increase of m beyond h_1 is still dominated by f spins and conduction electrons give the negative magnetization; this is due to the internal field via the Kondo-coupling J and note that the density of states shifts to the direction opposite to that expected in this weak-h regime. On the contrary, the property for the higher magnetic field up to the saturation h_2 is characterized by conduction electrons. In Fig. 1(c), the intra and intersite spin-spin correlations for the central i-th site are shown. At $h = 0$, the magnetic moments are mostly canceled by the incommensurate array of f spins, and the residual moments are screened by formation of the collective Kondo singlet in the small-J/t regime [6,12]. Even if h is switched on, the intra and intersite correlations shows minor change as long as $0 \leq h \leq h_1$. However, once h exceeds h_1, the intersite incommensurate correlation of f spins is destroyed abruptly to be the ferromagnetic one. On the contrary, the intrasite f-c singlet correlation survives even in the larger magnetic field. Consequently, it turns out that the rapid increase of m beyond $h_1 \sim T_{\rm K}$ is caused by the collapse of the intersite incommensurate correlation of f spins.

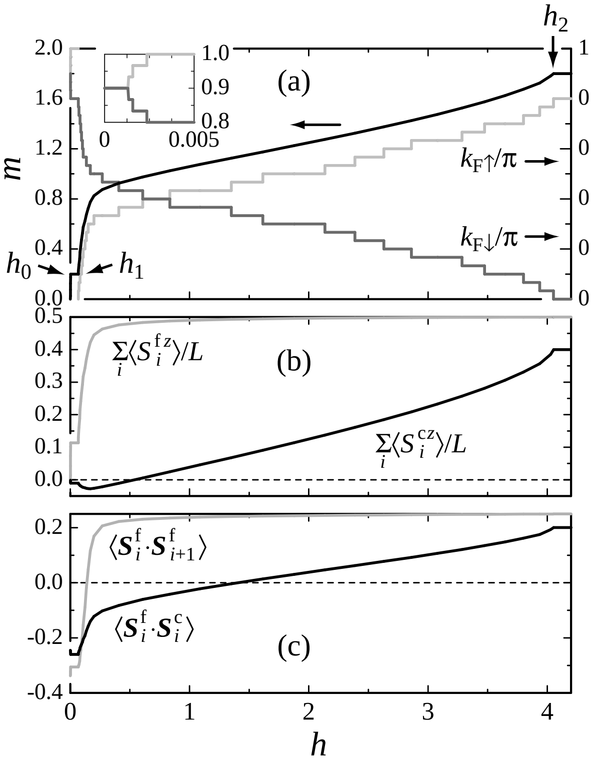

FIG. 1. (a) Magnetization curve and Fermi surfaces (b) $\sum_i\langle S_i^{fz}\rangle/L$ and $\sum_i\langle S_i^{cz}\rangle/L$ (c) intrasite correlation $\langle \mathbf{S}_i^f\cdot\mathbf{S}_i^c\rangle$ and intersite correlation $\langle \mathbf{S}_i^f\cdot\mathbf{S}_{i+1}^f\rangle$, under the magnetic field h for $t = 1$ and $J = 1$ at $n_c = 4/5$. The inset in (a) is the enlargement of the small-h regime for $k_{\rm F\uparrow}/\pi$ and $k_{\rm F\downarrow}/\pi$ (see text).

By the calculations for various $n_{\rm c}$, we find that the magnetization plateau appears at $m = 1 - n_{\rm c}$. This can be intuitively understood if we take the real-space picture which is relevant in the large-J/t limit: The number $L(1-n_c)$ is equivalent to the number of the hole whose site has an only f spin. For $0 \leq h \leq h_0$, these f spins are polarized by the magnetic field, in order to avoid the energy loss to destroy the intrasite f-c singlet correlation. As long as $h_0 \leq h \leq h_1$, this state is still stable so that the magnetization plateau appears. Once h exceeds h_1, the f-c singlet starts to be broken as shown above.

We now turn to the location of the Fermi surface. The Fermi wave number $k_{\rm F\sigma}$ for each spin defined as the singular point in the momentum distribution function is detected by the period of the Friedel oscillation [13]. The open boundary condition used in the present calculation works as the perturbation which induces the density oscillations: The one-particle charge density for conduction electrons under the open boundary condition is written as

$$\langle N^c(x)\rangle \sim A_\uparrow\frac{\cos(2k_{\rm F\uparrow}x)}{x^{\gamma_\uparrow}} + A_\downarrow\frac{\cos(2k_{\rm F\downarrow}x)}{x^{\gamma_\downarrow}} + B\frac{\cos[2(k_{\rm F\uparrow}+k_{\rm F\downarrow})x]}{x^{\gamma}}, \qquad (2)$$

where $\langle N^c(x)\rangle = \langle N^c_\uparrow(x)\rangle + \langle N^c_\downarrow(x)\rangle$ with $\langle N^c_\sigma(x)\rangle$ being the one-particle density with spin σ [14,15]. The spin density $\langle S^{cz}(x)\rangle = (\langle N^c_\uparrow(x)\rangle - \langle N^c_\downarrow(x)\rangle)/2$ has the same form as $\langle N^{\rm c}(x)\rangle$, but with different coefficients A_σ and B.

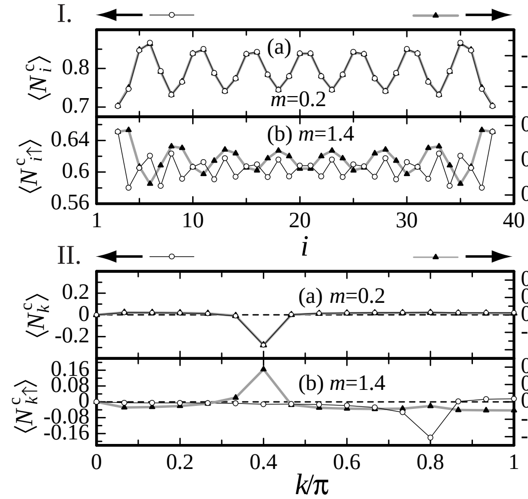

FIG. 2. One particle density in the real space (I) and its Fourier spectrum (II). (a) $m = 0.2$ and (b) $m = 1.4$ for $t = 1$ and $J = 2$ at $n_c = 4/5$. The Fourier transformation is carried out by using the central 30 sites.

As shown in Fig. 2I, we calculate $\langle N_i^c\rangle = \langle N_{i\uparrow}^c\rangle + \langle N_{i\downarrow}^c\rangle$ and $\langle S_i^{cz}\rangle = (\langle N_{i\uparrow}^c\rangle - N_{i\downarrow}^c\rangle)/2$ with $\langle N_{i\sigma}^c\rangle = \langle c_{i\sigma}^\dagger c_{i\sigma}\rangle$ for each magnetization. The Fermi wave number is derived from the peak structure in the Fourier spectrum of $\langle N_i^c\rangle$ and $\langle S_i^{cz}\rangle$ as in Fig. 2II. In Fig. 2I(a) we see that the holes are located mutually keeping the interval of 4 sites in the case of $m = 1/5$ which corresponds to the plateau. This configuration is detected by the peak structure at $2(k_{\rm F\uparrow} + k_{\rm F\downarrow}) = 2\pi/5 \pmod{2\pi}$ in Fig. 2II(a), which persists in its position even if m changes. Additionally, there appears the $2k_{\rm F\sigma}$ peak for each spin whose position depends on m. As m increases ($\gtrsim$1), the peak is detected more easily by $\langle N^c_{i\sigma}\rangle$ rather than by $\langle N^c_i\rangle$ and $\langle S^{cz}_i\rangle$. We see that the clear two peaks of $2k_{\mathrm{F}\uparrow}$ and $2k_{\mathrm{F}\downarrow}$ appear and also that the amplitude for $2(k_{\mathrm{F}\uparrow}+k_{\mathrm{F}\downarrow})$ becomes quite small in Fig. 2II(b). We show the $J=2$ data in Figs. 2(a) and 2(b), since the $J=1$ data contain the additional small peak which is not intrinsic as reported at $h=0$ [13]. The resultant $k_{\mathrm{F}\sigma}$ is shown in Fig. 1(a). At $h=0$ the Fermi wave number is given by $k_{\mathrm{F}\uparrow}=k_{\mathrm{F}\downarrow}=\pi(1+n_c)/2=9\pi/10$ [13]: Namely, the Fermi surface is large, which includes the contribution from f spins. As h increases from 0 to h_0, $k_{\mathrm{F}\uparrow}$ ($k_{\mathrm{F}\downarrow}$) increases (decreases) to π ($\pi n_c=4\pi/5$), and they remain the same as long as $h_0\le h\le h_1$. When h exceeds h_1, $k_{\mathrm{F}\uparrow}$ increases from 0 and $k_{\mathrm{F}\downarrow}$ decreases from πn_c. When h reaches the saturation field h_2, we obtain $k_{\mathrm{F}\uparrow}=\pi n_c=4\pi/5$ and $k_{\mathrm{F}\downarrow}=0$, which are equal to the small Fermi surfaces of the completely polarized conduction bands decoupled to f spins.

We confirmed that the Fermi surfaces obtained with use of eq. (2) and the magnetization derived from the minimization of the total energy satisfy the following relation; $k_{\mathrm{F}\sigma}/\pi=(1+n_c\pm m)/2$, where $\sigma=\uparrow$ ($\downarrow$) corresponds to $+(-)$ in the right hand side. This means that there is no phase transition and that the Luttinger's sum rule holds in a magnetic field. The expression of $k_{\mathrm{F}\sigma}$ is consistent with the argument on the basis of the generalized Lieb-Schultz-Mattis theorem [16]. The important point is that the Fermi surface is always *large*, which involves the contribution from f spins, whereas the crossover from large to small Fermi surfaces is observed [17].

In order to analyze the crossover from large to small Fermi surfaces in detail, let us consider the PAM:

$$H_{\mathrm{PAM}}=-t\sum_{i\sigma}\left(c^\dagger_{i\sigma}c_{i+1\sigma}+\mathrm{H.c.}\right)+\varepsilon_f\sum_{i\sigma}n^f_{i\sigma}$$
$$+V\sum_{i\sigma}\left(f^\dagger_{i\sigma}c_{i\sigma}+\mathrm{H.c.}\right)+U\sum_i n^f_{i\uparrow}n^f_{i\downarrow}. \qquad (3)$$

The KLM is the effective model derived from the PAM in the regime of $U\gg\pi\rho(0)V^2$ under the symmetric condition $\varepsilon_f+U/2=0$, where $\rho(0)$ is the density of states of conduction electrons at the Fermi energy. Finite U makes the effective f level shifted up to the Fermi energy where the Kondo resonance responsible for the heavy quasi-particle band arises. From the viewpoint of the adiabatic continuation, we consider the simplest case of $\varepsilon_f=-U/2=0$ in eq. (3). In Fig. 3, the solid curve represents the magnetization of the PAM with the Zeeman term $-h\sum_i(S^{fz}_i+S^{cz}_i)$ for the doped ($n=n_f+n_c=9/5$) case.

For $h^*_0\le h\le h^*_1$ the plateau at $m=2-n$ appears as a consequence of the hybridization gap: $\Delta=-2t+2\sqrt{t^2+V^2}$. Here the critical fields h^*_i ($i=0,1$) are given by

$$h^*_i=t\left\{(-1)^i-\cos(n\pi)-(-1)^i\sqrt{1+(V/t)^2}\right.$$
$$\left.+\sqrt{\cos^2(n\pi)+(V/t)^2}\right\},$$

and the saturation field h^*_2 by $h^*_1+t[1+\cos(n\pi)]$. Namely, the plateau appears as long as the bottom of the upper empty band with majority spin becomes lower than the top of the lower filled band with minority spin as h increases. In order to separate the contribution from conduction electrons, we also show the magnetization for $V=0$, setting $n_f=1$ and $n_c=4/5$. Additionally, the discrete data of $J=1$ and 2 in the KLM at $n_c=4/5$ are shown, whose horizontal axis is scaled by h_1. To facilitate the comparison between the PAM and the KLM, the magnetization curve of the PAM is also scaled by h^*_1 and we choose the hybridization V fixing $t=1$ in eq. (3) so that h^*_1 is equal to h_1 of the KLM. The $V=0$ case is scaled by the same unit of the corresponding $V\neq0$ case. Note that the data for the PAM are just located on those for the KLM for $0\le h\le h_1$. In Fig. 3, the solid arrow indicates the magnetic field on which the sign of $\langle\mathbf{S}^f_i\cdot\mathbf{S}^c_i\rangle$ changes in the KLM (see Fig.1(c)).

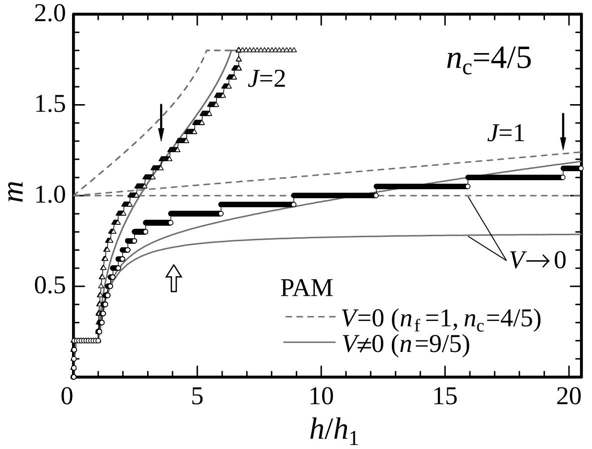

FIG. 3. Magnetization of the KLM for $n_c=4/5$ and of the PAM for $n=9/5$, with $t=1$. The dashed line represents the $V=0$ case of the PAM with $n_f=1$ and $n_c=4/5$. Each data for $V\neq0$ and $V=0$ of the PAM is scaled by h^*_1, where h^*_1 is set to be equal to h_1 of the KLM. The solid arrows show the point where $\langle\mathbf{S}^f_i\cdot\mathbf{S}^c_i\rangle$ of the KLM changes the sign. The open arrow indicates the crossover point from large to small Fermi surfaces (see text).

As for the PAM, we see in Fig. 3 that the magnetization for finite V approaches that for $V=0$ with $n_f=1$ and $n_c=4/5$ as h increases. Namely, the crossover from f to conduction electrons which gives the dominant contribution to the magnetization as well as the Fermi surfaces occurs beyond h^*_1. Note that, even in the large-h regime where the Fermi surface is dominated by conduction electrons, f electrons are coupled to conduction electrons; f electrons are always itinerant, but *not* localized. Since Δ is reduced to be the order of $T_{\mathrm{K}}=2t\exp\{-U/(8\rho(0)V^2)\}$ by finite U, the range where f electrons give the main contribution to the magnetization process will be drastically reduced by the many-body effects. As seen in the $V \to 0$ limit, the Fermi surface can be close to that of conduction electrons beyond slightly larger h than $h_1^* \sim T_{\rm K}$ as indicated by the open arrow. The difference of the size of the Fermi surface between $V \to 0$ and $V = 0$ cases around the open arrow becomes small as n approaches 2 (half filling). Similarly, we expect that the crossover will be observed around $h_1 \sim T_{\rm K}$ in the KLM in the realistic $J/t \to 0$ case near half filling, where the intrasite f-c singlet correlation remains.

As seen in Fig. 3, the general behavior of the PAM is similar to that of the KLM. This implies that the k-space (band) picture for the PAM continuously connects with the real-space picture for the KLM explained in Fig. 1. Namely, for the PAM the smaller end of the plateau (h_0^*) is associated with the slope (i.e., velocity) of the lower hybridized band whose component is dominated by f electrons, and the larger one (h_1^*) connects to the hybridization gap Δ as n approaches to 2. The correspondence between the above picture and the result of the KLM leads us to find the following meaning of the magnetization plateau in the KLM: The smaller end of the plateau (h_0) is associated with the velocity of the effective carriers whose main component is unscreened f spins with density $1 - n_c$, and the larger one (h_1) is related to the intrasite f-c singlet correlation, which connects to the spin gap $\Delta_{\rm s}$ as n_c approaches 1. These two characteristic energies are considered to be related to the coherence temperature T^* and the Kondo temperature $T_{\rm K}$; the former and the latter are often observed as the characteristic temperatures which give T^2 and $\log T$ behaviors in the resistivity, respectively in heavy electron compounds. The quasi-particle picture with respect to the KLM obtained here via the response to the magnetic field is consistent with recent calculations of dynamical and finite-temperature quantities without h by N. Shibata, *et al.* [18]

When realistic factors which should enter are taken into account, the plateau tends to be smeared; the difference of g factors between f and conduction electrons, anisotropy of the hybridization, the dispersion of the f band, etc. [19] Hence, the shape of m itself for $0 \le h \le h_1$ changes according to these factors. However, physics shown here offers significant pictures to understand the magnetization process of heavy electron compounds. As for CeRu$_2$Si$_2$, it was confirmed that there is no first order phase transition at $H_{\rm M}$ and the electronic state changes continuously [20]. This suggests that the crossover from large to small Fermi surfaces occurs with the f-electron number involved. Simultaneously, we pointed out that the localization of f electrons above $H_{\rm M}$ is not necessary to interpret both the results of the dHvA experiment [2] and the band structure calculations [3]. Furthermore, we show the rapid increase of the magnetization due to the collapse of the intersite correlation of f spins and the toughness of the intrasite f-c singlet correlation. These tendencies are observed by the neutron measurement [4].

In conclusion, we show the fundamental mechanism of the magnetization process in the one-dimensional KLM and shed light on the heavy quasi-particle picture via the response to the magnetic field.

The author would like to thank Y. Kuramoto for bringing my attention to this problem as well as the fruitful discussions. The author is grateful to N. Shibata for sending his data prior to the publication as well as useful discussions. Thanks are also due to H. Tsunetsugu, H. Yamagami, M. Oshikawa and O. Sakai for valuable discussions. A part of the numerical calculation was performed by VPP500 at the Supercomputer Center of the ISSP, Univ. of Tokyo.

---

* Electronic address: watanabe@cmpt01.phys.tohoku.ac.jp

[1] J. M. Mignot, *et al.*, J. Magn. & Magn. Mater. **76**&**77**, 97 (1988).

[2] H. Aoki, *et al.*, Phys. Rev. Lett. **71**, 2110 (1993); H. Aoki, *et al.*, J. Phys. Soc. Jpn. **62**, 3157 (1993).

[3] H. Yamagami and A. Hasegawa, J. Phys. Soc. Jpn. **61**, 2338 (1992); H. Yamagami and A. Hasegawa, J. Phys. Soc. Jpn. **62**, 592 (1993).

[4] J. Rossat-Mignod, *et al.*, J. Magn. & Magn. Mater. **76**&**77**, 376 (1988).

[5] K. Ueda, J. Phys. Soc. Jpn. **58**, 3465 (1989).

[6] K. Yamamoto and K. Ueda, J. Phys. Soc. Jpn. **59**, 3284 (1990).

[7] T. Saso and M. Ito, Phys. Rev. B**53**, 6877 (1996).

[8] H. M. Carruzzo and C. Yu, Phys. Rev. B**53**, 15377 (1996).

[9] K. Tsutsui, *et al.*, Physica B **230-232**, 421 (1997).

[10] S. R. White, Phys. Rev. Lett. **69** 2863 (1992); S. R. White, Phys. Rev. B **48**, 10345 (1993).

[11] H. Tsunetsugu, Y. Hatsugai and K. Ueda, Phys. Rev. B**46**, 3175 (1992); N. Shibata, *et al.*, Phys. Rev. B**53**, R8828 (1996).

[12] H. Tsunetsugu, M. Sigrist and K. Ueda, Phys. Rev. B **47**, 8345 (1993).

[13] N. Shibata, *et al.*, Phys. Rev. B **54**, 13495 (1996); N. Shibata, A. Tsvelik and K. Ueda, Phys. Rev. B **55**, 1 (1997).

[14] J. L. Cardy, Nucl. Phys. B**240**, 514 (1984).

[15] G. Bedürftig, *et al.*, Phys. Rev. B **58**, 10225 (1998).

[16] M. Yamanaka, M. Oshikawa and I. Affleck, Phys. Rev. Lett. **79**, 1110 (1997).

[17] At the saturation with $m = 1 + n_c$, the Fermi surfaces can be equal to the small ones; $2k_{{\rm F}\uparrow} = 2\pi(1+n_c) = 2\pi n_c$ and $2k_{{\rm F}\downarrow} = 0$.

[18] N. Shibata and H. Tsunetsugu, J. Phys. Soc. Jpn. **68**, 744 (1999); N. Shibata and H. Tsunetsugu, preprint(cond-mat/9907416).

[19] S. M. M. Evans, Europhys. Lett. **17**, 469 (1992).

[20] T. Sakakibara, *et al.*, Phys. Rev. B **51**, 12030 (1995).